Check for updates

Furfural-derived 5-alkoxy-2(5*H*)-furanones as cationically copolymerizable cyclic hemiacetal esters†

Naoki Higashibata, Sadahito Aoshima [ID] and Arihiro Kanazawa [ID] *

We have focused on cyclic hemiacetal esters as monomers that undergo cationic ring-opening copolymerization. In this study, we investigated the cationic ring-opening copolymerization of 5-alkoxy-2(5*H*)-furanones (ROFOs), which are cyclic hemiacetal esters synthesized from a plant-derived compound (furfural) *via* photochemical reaction. ROFOs did not undergo cationic homopolymerization, while copolymerization with oxiranes successfully proceeded to yield polymers with ester and acetal moieties in the main chain. In addition, cationic terpolymerization of vinyl ether (VE), oxirane, and ROFO proceeded *via* highly selective crossover reactions, resulting in sequence-controlled terpolymers with VE$_n$–oxirane$_m$–ROFO-type periodic structures. The co- and terpolymers could be degraded by acid hydrolysis *via* the scission of the acetal moieties in the main chain. The copolymers obtained from ROFO have β-substituted acrylate structures in the main chain; hence, the polymers could be modified by the thiol–ene reaction.

Introduction

Polymerizability of cyclic monomers in ring-opening polymerization (ROP) is governed by several factors, such as ring strain, reactivity of propagating species, and stability of the structures resulting from propagation reactions.[1] Cyclic ethers including oxiranes and oxetanes undergo cationic ROP *via* the oxonium ion-mediated propagation reactions, which relies on the liberation of ring strain as a driving force.[2–4] In addition, cyclic monomers that do not exhibit homopolymerizability potentially undergo copolymerization when appropriate comonomers are used. For example, nonhomopolymerizable cyclic acetals[5] undergo cationic copolymerization with vinyl monomers such as vinyl ethers (VEs) and styrene derivatives.[6,7] The crossover reaction from a cyclic acetal to a vinyl monomer occurs *via* the carbocation (oxocarbenium ion) generation through the ring-opening of the cyclic acetal-derived oxonium ion.

Cyclic hemiacetal esters have a carbon atom adjacent to both ester and alkoxy groups in a ring, which is responsible for the characteristic polymerizability. Coordination–insertion-

type ROP of 1,3-dioxolan-4-ones (DOLOs), which are five-membered cyclic hemiacetal esters, was reported to proceed by a metal complex catalyst, while a carbonyl compound eliminates from the propagating end, resulting in not poly(DOLO)s but poly(α-hydroxy acid)s, such as polylactide.[8,9] Copolymerization of DOLOs and cyclic esters was also reported to proceed.[10,11] We previously reported that DOLOs did not undergo cationic homopolymerization but underwent cationic copolymerization with oxiranes.[12] An alkoxy group-adjacent carbocation (oxocarbenium ion), which has a structure similar to that of a VE-derived carbocation, is most likely generated *via* the ring-opening reaction that occurred after the reaction between an oxirane-derived oxonium ion and the carbonyl group of a DOLO (Scheme 1A). In addition, cationic copolymerization of VE and DOLO did not proceed, while terpolymerization proceeded when VE, oxirane, and DOLO were combined. Moreover, we demonstrated that 3-alkoxyphthalides (ROPTs; Scheme 1A), which have a fused aryl ring in a five-membered cyclic hemiacetal ester structure, underwent cationic copolymerization with oxiranes *via* more frequent crossover reactions than the DOLO case.[13] ROPTs also did not undergo cationic homopolymerization. Unlike these five-membered cyclic hemiacetal esters, six- and seven-membered counterparts were reported to undergo cationic homopolymerization.[14,15] Bicyclic compounds with a five-membered cyclic hemiacetal structure also undergo cationic homopolymerization.[16]
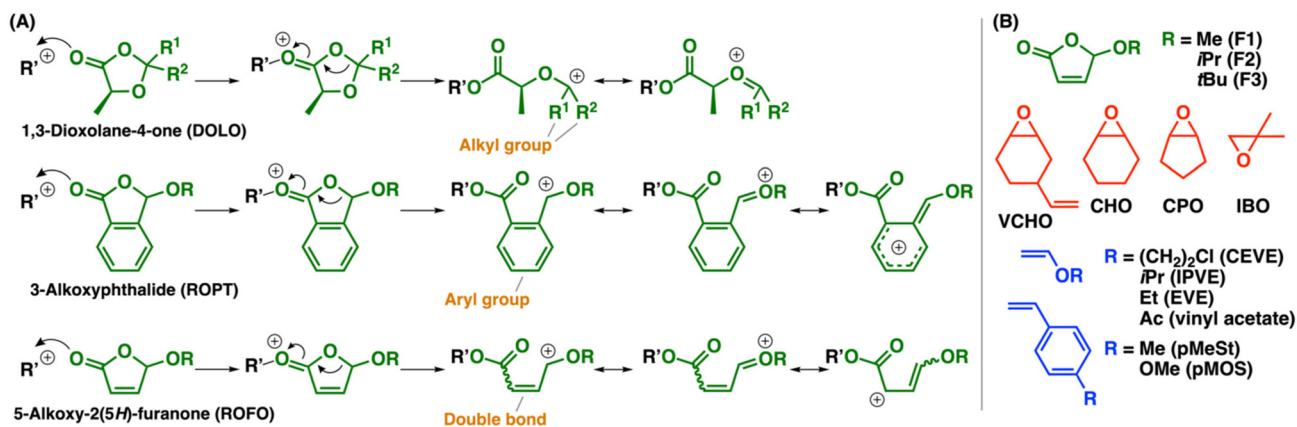
As potentially polymerizable cyclic hemiacetal esters, we focused on 5-alkoxy-2(5*H*)-furanones (ROFOs), which are syn-

---

Department of Macromolecular Science, Graduate School of Science, Osaka University, Toyonaka, Osaka 560-0043, Japan.
E-mail: kanazawaa11@chem.sci.osaka-u.ac.jp

Scheme 1 (A) Propagating species generated from DOLO, ROPT, or ROFO. (B) Monomers used in this study.

thesized from furfural by the photochemical reaction.[17–20] ROFOs have a five-membered cyclic hemiacetal structure with a carbon–carbon double bond in the ring. This structure corresponds to a β-substituted acrylate. Indeed, ROFOs were reported to undergo radical copolymerization with vinyl monomers through the reaction of a radical species and the double bond.[21,22] However, the use of ROFOs as cyclic monomers for ROP was not previously reported as far as we know. When the carbonyl group of an ROFO reacts with a cationic species, subsequent ring-opening reaction is expected to result in a carbocation adjacent to both alkoxy group and carbon–carbon double bond (Scheme 1A). This carbocation has a structure different from those of the DOLO-derived, alkoxy group-adjacent carbocation and the ROPT-derived, alkoxy group- and aryl group-adjacent carbocation;[12,13] hence, ROFOs are expected to exhibit polymerizability different from those of DOLOs and ROPTs.

In this study, we examined the cationic polymerization of ROFOs with a methoxy, isopropoxy, or *tert*-butoxy group (Scheme 1B). Cationic homopolymerization of ROFOs did not proceed at all, whereas cationic copolymerization with oxiranes successfully proceeded to yield copolymers with acetal, ester, and carbon–carbon double bond moieties in the main chain. Interestingly, the ROFO-derived carbocation underwent highly selective reaction with an oxirane monomer, resulting in a single structure among the four possible structures associated with carbocation conjugation and *cis–trans* configuration. Cationic terpolymerization of ROFOs with VEs and oxiranes also proceeded efficiently. In addition, the obtained copolymers could be modified by the thiol–ene reaction of the ROFO-derived β-substituted acrylate moieties in the main chain.

Results and discussion

Synthesis of ROFOs

ROFOs were synthesized from furfural.[17–20] A solution of furfural in methanol was bubbled with air under irradiation with a white LED floodlight in the presence of rose bengal, resulting

in 5-hydroxy-2(5H)-furanone. 5-Methoxy-2(5H)-furanone (F1) and 5-isopropoxy-2(5H)-furanone (F2) were synthesized by the reaction of 5-hydroxy-2(5H)-furanone in methanol and 2-propanol, respectively. 5-*tert*-Butoxy-2(5H)-furanone (F3) was synthesized from 5-hydroxy-2(5H)-furanone by the reported method.[22] See the Experimental section in the ESI† for the details of monomer synthesis.
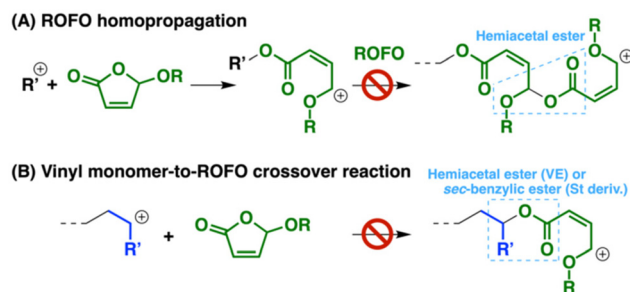
Cationic homopolymerization of ROFOs

Cationic homopolymerization of ROFOs was examined with $B(C_6F_5)_3$ or $GaCl_3$ as Lewis acid catalysts at different monomer concentrations and temperatures. However, ROFOs were not consumed at all under any conditions examined (entries 1–5 in Table 1). DOLOs and ROPTs also did not undergo homopolymerization in our previous studies.[12,13] The inertness of the five-membered cyclic hemiacetal esters in cationic homopolymerization is likely derived from both low ring-strain and ineffective generation of a hemiacetal ester moiety *via* the homopropagation reaction (Scheme 2A).

Table 1 Cationic homopolymerization of ROFOs and copolymerization with vinyl monomers[a]

				Conv. (%)	
Entry	ROFO	Vinyl monomer	Time (h)	ROFO	Vinyl
1	F1	—	166	0	—
2[b]	F1	—	96	0	—
3[c]	F1	—	96	0	—
4	F2	—	120	0	—
5	F3	—	72	0	—
6	F1	CEVE	166	0	0
7	F1	pMeSt	24	0	0
8	F1	pMOS	24	0	56
9	F2	CEVE	120	0	7
10	F3	CEVE	72	0	2

[a] $[ROFO]_0 = 0.75$ M, [vinyl monomer]$_0$ = 0 or 0.75 M, $[B(C_6F_5)_3]_0 = 3.0$ mM (except for entry 3), in dichloromethane at −78 °C (except for entry 2). [b] At 0 °C. [c] $GaCl_3$ (4.0 mM) was used instead of $B(C_6F_5)_3$.

(A) ROFO homopropagation

(B) Vinyl monomer-to-ROFO crossover reaction

Scheme 2 (A) Homopropagation reaction of ROFO and (B) crossover reaction from a vinyl monomer to ROFO.

Cationic copolymerization

Cationic copolymerization of 2-chloroethyl VE (CEVE) and ROFOs was ineffective (entries 6, 9, and 10 in Table 1), which is similar to the DOLO case.[12] Inefficient generation of a hemiacetal ester moiety by the crossover reaction from VE to ROFO is likely responsible for the inertness of ROFOs in the copolymerization with VEs (Scheme 2B). Styrene derivatives [*p*-methylstyrene (pMeSt) and *p*-methoxystyrene (pMOS)] were also ineffective as comonomers for copolymerization with ROFOs (entries 7 and 8).

Unlike unsuccessful homopolymerization and copolymerization with VEs, ROFOs were demonstrated to undergo cationic copolymerization with oxiranes. When F1 was copolymerized with VCHO using $B(C_6F_5)_3$ as a catalyst, both monomers were consumed to reach F1 and VCHO conversion of 57% and 11%, respectively, in 1 min (entry 1 in Table 2). An obtained polymer had an M_n value of 17.8×10^3 (Fig. 1A, black). ^{1}H NMR analysis suggested that the copolymer was produced by the crossover reactions between F1 and VCHO (Fig. 2A). An acetal moiety was generated *via* the crossover reaction from F1 to VCHO although the acetal peak (peak 11) partly overlapped with the peak of the double bonds in the main chain (peak 10) at 6.0–6.3 ppm. An ester moiety was generated *via* the cross-

over reaction from VCHO to F1 although the ester-adjacent methine peak (peak 8) also overlapped with the peaks of the VCHO-derived vinyl groups (peaks 6 and 7). The assignments of peaks shown in Fig. 2A were confirmed by ^{13}C and 2D NMR analyses (Fig. S1–S4†). From the integral ratios of the peaks in the ^{1}H NMR spectrum, the average number of VCHO/F1 units per block was calculated to be 5.4/1.0, respectively. The number of VCHO units per block decreased as the polymerization proceeded (entry 2, 3.6/1.0 for VCHO/R1) because of the faster decrease in the amount of VCHO than that of F1 during polymerization.

The VCHO–F1 copolymer has acetal moieties in the main chain; hence, the copolymer was degraded into oligomers by acid hydrolysis with HCl. The M_n value decreased from 17.8×10^3 to 1.2×10^3, while keeping a unimodal distribution (Fig. 1A, purple), indicating that acetal moieties were statistically located in the original copolymer. In the ^{1}H NMR spectrum (Fig. 2B), the peaks of the acetal and carbon–carbon double bond moieties at 6.0–6.3 ppm disappeared and instead peaks assigned to an alkenal structure[23] appeared (peaks 12–14), which is consistent with the scission of the acetal moiety adjacent to the double bond.

The copolymerization mechanism is explained as follows: the polymerization starts from the interaction between $B(C_6F_5)_3$ and VCHO or ROFO and/or a proton derived from the reaction between adventitious water and $B(C_6F_5)_3$. The homopropagation reaction of VCHO proceeds *via* the oxonium ion-mediated cationic ring-opening mechanism. An ROFO monomer reacts with the VCHO-derived oxonium ion through the attack of the carbonyl oxygen on the carbon atom of the three-membered ring moiety in the oxonium ion (Scheme 3A) in a manner similar to the cases of other cyclic hemiacetal esters (DOLOs and ROPTs).[12,13] Subsequently, the ring-opening of the ROFO-derived oxonium ion occurs to generate a carbocation adjacent to the alkoxy group, which has a structure of an oxocarbenium ion. This crossover reaction results in an ester moiety in the main chain (Scheme 3B). The homopro-

Table 2 Cationic copolymerization of VCHO and ROFOs[a]

Entry	ROFO	Time (min)	Conv. (%)		$M_n \times 10^{-3\ b}$	$M_w/M_n\ ^b$	Average no. of monomer units per block[c]	
			VCHO	ROFO			VCHO	ROFO
1	F1	1	57	11	17.8	2.40	5.4	1.0
2	F1	3	82	23	13.0	2.22	3.6	1.0
3	F2	1	80	26	21.2^d	1.79^d	3.2	1.0
4	F3	7.5	74	25	13.8^d	3.12^d	3.0	1.0

[a] $[VCHO]_0 = 0.75$ M, $[ROFO]_0 = 0.75$ M, $[B(C_6F_5)_3]_0 = 1.0$ (entries 1 and 2) or 3.0 (entries 3 and 4) mM, in dichloromethane at −78 °C. [b] Determined by GPC (polystyrene calibration). [c] Calculated by ^{1}H NMR. [d] Values for a main peak.
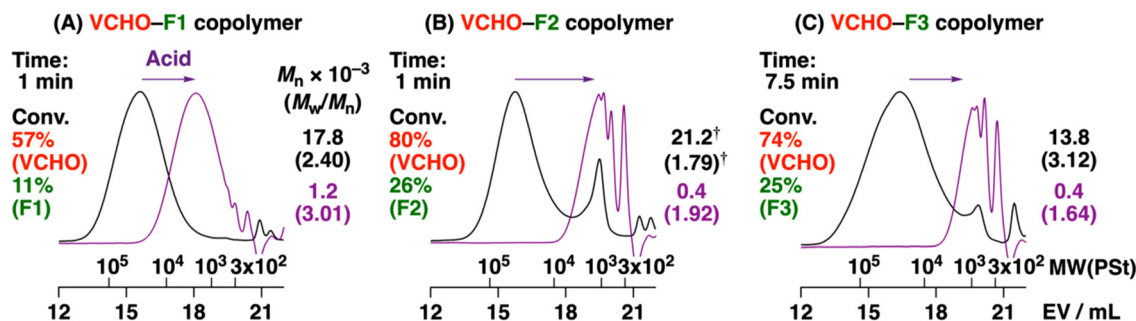
Fig. 1 MWD curves of (A) VCHO−F1 (entry 1 in Table 2), (B) VCHO−F2 (entry 3), and (C) VCHO−F3 (entry 4) copolymers (black) and their acid hydrolysis products (purple). See Table 2 for the polymerization conditions.† Values for a main peak.
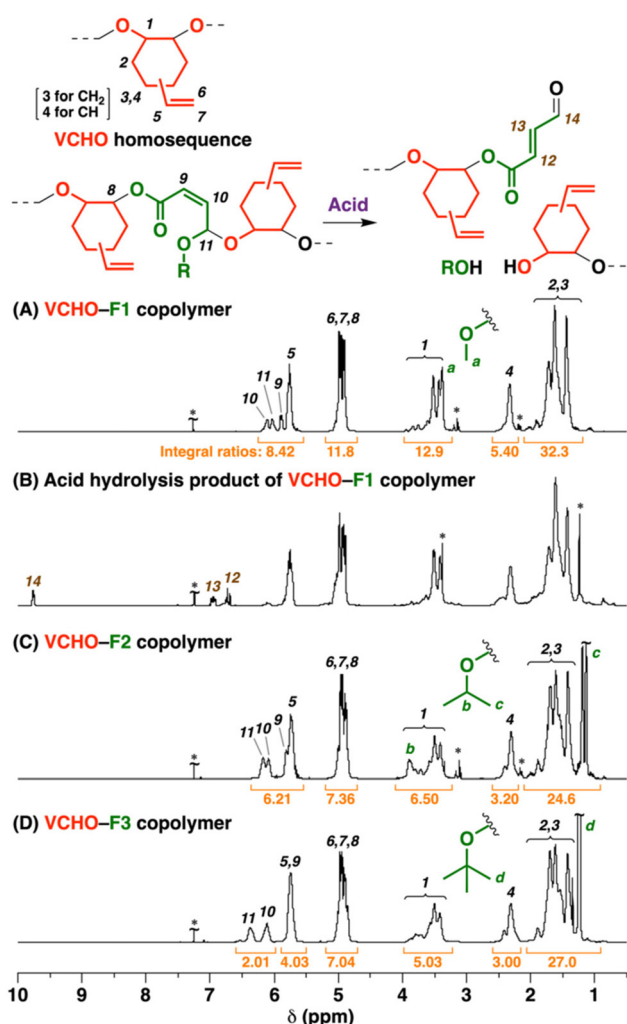

Fig. 2 ^{1}H NMR spectra of (A) VCHO−F1 copolymer (entry 1 in Table 2; Fig. 1A), (B) its acid hydrolysis product (purple curve in Fig. 1A), (C) VCHO−F2 copolymer (entry 3 in Table 2; Fig. 1B), and (D) VCHO−F3 copolymer (entry 4 in Table 2; Fig. 1C, after reprecipitation in methanol). In CDCl₃ at 30 °C. The integral ratios of unnecessary peaks (water, residual monomer, *etc.*) were subtracted. * CHCl₃, residual monomer, 1,2-dimethoxyethane, *etc.*
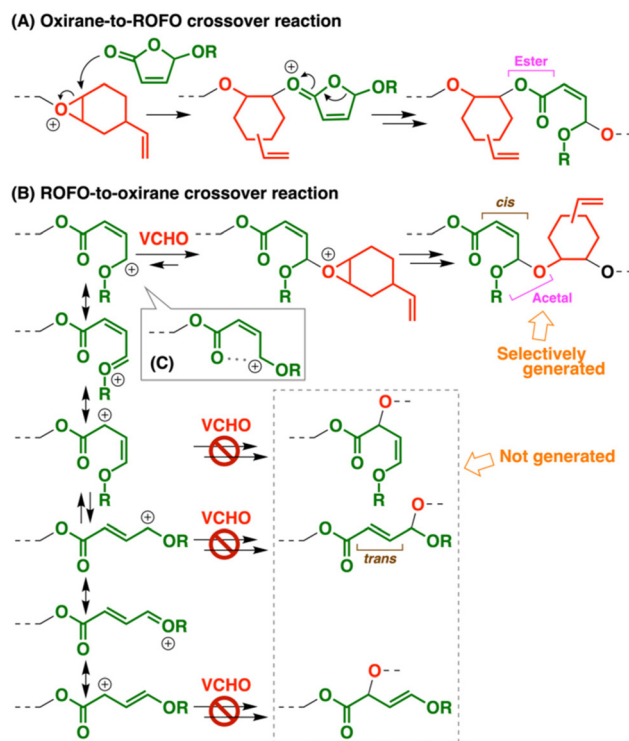
Scheme 3 (A) Crossover reaction from VCHO to ROFO, (B) crossover reaction from ROFO to VCHO, and (C) possible interaction of a carbocation with the carbonyl group.

pagation reaction of ROFOs does not proceed (Scheme 2A); hence, the carbocation reacts with a VCHO monomer, which is followed by the VCHO homopropagation. An acetal moiety is generated in the main chain by the crossover reaction from ROFO to VCHO. The monomer reactivity ratios of VCHO and F1 were determined to be 4.7 and 0, respectively, by the Meyer–Lowry method (Fig. S5 and Table S1†).[24,25] The values are consistent with the average number of monomer units per block in the copolymer chains.

Four different ROFO-derived structures are potentially generated in the main chain because the ROFO-derived carbocation has an adjacent carbon–carbon double bond (Scheme 3B). As expected from the resonance structure and the *cis–trans* configurations, this carbocation potentially reacts with VCHO at not only the alkoxy group-adjacent carbon atom but also the ester-adjacent carbon atom. In addition, *cis-* and *trans*-carbon–carbon double bonds are potentially generated after the reaction with VCHO. Among the four possible structures, the copolymer chain was found to exclusively have *cis*-double bonds derived from the reaction of the alkoxy group-adjacent carbon atom and VCHO, which was confirmed by the comparison of the ^{1}H NMR spectrum with those of the corresponding compounds[26] (also confirmed by *cis–trans* isomerization during the radical reaction; see below). The superiority of an alkoxy group-adjacent carbocation (oxocarbenium ion) in the resonance structures and the interaction between the carbonyl group with a cationic center (Scheme 3C) are possible causes of the highly selective reaction.

F2 and F3, which are isopropoxy and *tert*-butoxy counterparts of F1, respectively, also underwent cationic copolymerization with VCHO, resulting in copolymers with M_n values over 10^4 (entries 3 and 4 in Table 2; Fig. 1B and C). The average number of VCHO units per block of the copolymers, which was calculated from ^{1}H NMR spectra (Fig. 2C and D; see Fig. S6–S9† for the ^{13}C and 2D NMR spectra of the VCHO–F2 copolymer), was comparable among the three ROFOs when the samples of similar VCHO conversion were compared (entries 2–4 in Table 2). Small peaks were detected in the MWD curves of the F2- and F3-derived copolymers (Fig. 1B and C). These peaks are likely assigned to cyclic oligomers from the results of matrix-assisted laser desorption/ionization time-of-flight mass spectrometry (MALDI-TOF-MS) analysis (Fig. S10†).

Other oxiranes than VCHO were also copolymerized with ROFOs. Copolymers were generated by the copolymerization of CHO with F1, F2, or F3 (entries 1–3 in Table 3, Fig. S11 and S12†), while the MWs of the polymers were lower and the average number of oxirane units per block was larger than the VCHO counterparts. The copolymerization of CPO with ROFOs proceeded at much slower rates than those of the copolymerization with VCHO or CHO (entries 4–6 in Table 3, Fig. S11 and S13†). The MWs and the crossover frequency were comparable to those of the copolymerization with CHO. Unlike these two oxiranes, the use of IBO as an oxirane comonomer resulted in oligomers in the copolymerization with F1 or F2 (entries 7 and 8 in Table 3, Fig. S11†).

Comparison of cyclic hemiacetal esters

ROFOs exhibited higher and smaller reactivity than ROPTs and DOLOs did, respectively,[12,13] as indicated by the number of oxirane units per block in the copolymers (Fig. 3). The nucleo-
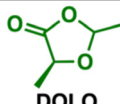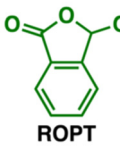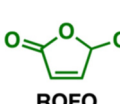

Fig. 3 Comparison of the M_n values and the average number of monomer units per block of the copolymers obtained by the copolymerization of oxiranes and cyclic hemiacetal esters ([oxirane]$_0$ = 0.75 M, [cyclic hemiacetal ester]$_0$ = 0.75 M, [B(C$_6$F$_5$)$_3$]$_0$ = 1.0 or 3.0 mM), in dichloromethane at −78 °C. Ref. 12 and 13 for the DOLO and ROPT data, respectively (except for the DOLO–CPO copolymer [unpublished data]).

Table 3 Cationic copolymerization of ROFOs with CHO, CPO, or IBO[a]

| Entry | Oxirane | ROFO | Time | Conv. (%) | | $M_n \times 10^{-3}$ [b] | M_w/M_n [b] | Average no. of monomer units per block[c] | |
				Oxirane	ROFO			Oxirane	ROFO
1	CHO	F1	30 s	90	11	10.6	2.06	8.3	1.0
2		F2	1 min	43	9	7.9	2.55	6.0	1.0
3		F3	5 min	93	21	2.1	2.61	4.4	1.0
4	CPO	F1	20 h	59	8	6.0	1.96	7.0	1.0
5		F2	68 h	35	5	4.3	1.35	6.2	1.0
6		F3	50 h	30	5	4.3	1.59	7.2	1.0
7	IBO	F1	45 h	2	<1	0.8	1.71	—	—
8		F2	144 h	4	1	0.4	1.32	—	—

[a] [Oxirane]$_0$ = 0.75 M, [ROFO]$_0$ = 0.75 M, [B(C$_6$F$_5$)$_3$]$_0$ = 3.0 (except for entries 1 and 2) or 1.0 (entries 1 and 2) mM, in dichloromethane at −78 °C. [b] Determined by GPC (polystyrene calibration). [c] Calculated by ^{1}H NMR.
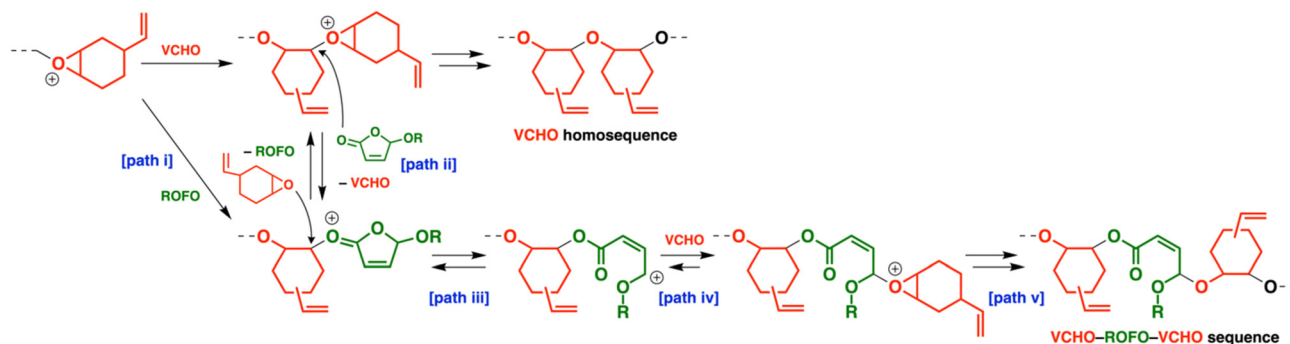
Scheme 4 Plausible processes of the propagation reactions.

philicity of cyclic hemiacetal esters (paths i and ii in Scheme 4; VCHO–ROFO copolymerization as an example), the ring-opening rate of the oxonium ion (path iii), and/or the reaction rate of the carbocation and an oxirane (path iv and v) are likely responsible for the difference in the incorporated ratios of cyclic hemiacetal esters in copolymers. This is considered assuming that the cyclic hemiacetal ester-derived oxonium ion formation (path ii in Scheme 4), the ring-opening reaction (path iii), and the oxirane-derived oxonium ion formation by the reaction of the carbocation and oxirane (path iv) are reversible processes. The difference of the carbocation stability (Scheme 1A) potentially affects the frequency of carbocation generation, the reverse reaction from the carbocation to the oxonium ion, and the reaction of a carbocation with an oxirane (paths iii and iv).

ROFOs and ROPTs exhibited higher reactivity than DOLO did, while the copolymerization of ROFOs or ROPTs with IBO was not effective unlike that of DOLO (Fig. 3).[12] The ROFO- and ROPT-derived carbocations, which have double bond- and aryl group-conjugated structures, respectively (Scheme 1A), are likely not suited for the reaction with IBO.

Cationic terpolymerization

Cationic copolymerization of VEs and ROFOs did not proceed as explained above, while ROFOs potentially undergo cationic terpolymerization with VEs and oxiranes, like the DOLO and ROPT cases,[12,13] because the ROFO-derived carbocation (oxocarbenium ion), which is generated by the reaction with an oxirane, is expected to react with a VE monomer. We therefore conducted terpolymerization of IPVE, VCHO, and ROFOs under similar conditions to those for the copolymerization of VCHO and ROFOs. A higher concentration of IPVE than that of VCHO was used to facilitate crossover reactions from VCHO to ROFO. As a result, polymers with M_n values of 11.5, 8.0, or 28.1 $\times 10^3$ were obtained from F1, F2, or F3, respectively (entries 1–3 in Table 4; Fig. 4). ^{1}H NMR analysis of the products suggested that IPVE, VCHO, and ROFOs were incorporated into polymer chains (Fig. 5). From the integral ratios of key peaks (explained below), the average number of IPVE/VCHO/ROFO units was calculated to be 7.1/1.8/1.0, 5.1/1.9/1.0, and 6.7/1.3/1.0 for F1, F2, and F3, respectively, indicating that terpolymers were successfully produced by the crossover reactions

Table 4 Cationic terpolymerization of VE, VCHO, and ROFO[a]

Entry	Monomer		Time (min)	Conv. (%)			$M_n \times 10^{-3}$ [b]	M_w/M_n [b]	Average no. of monomer units per block[c]			Propagation from ROFO[c] (%)	
	VE	ROFO		VE	VCHO	ROFO			VE	VCHO	ROFO	To VE	To VCHO
1	IPVE	F1	2	50	48	7	11.5	2.44	7.1	1.8	1.0	71	29
2	IPVE	F2	20	53	62	8	8.0	2.06	5.1	1.9	1.0	94	6
3	IPVE	F3	20	76	59	11	28.1	1.81	6.7	1.3	1.0	>99	<1
4	EVE	F3	15	10	50	8	5.4	2.74	1.3	1.6	1.0	98	2

[a] $[VE]_0$ = 0.80 M, $[VCHO]_0$ = 0.20 M, $[ROFO]_0$ = 0.80 M, $[B(C_6F_5)_3]_0$ = 1.0 mM, in dichloromethane at −78 °C. [b] Determined by GPC (polystyrene calibration). [c] Calculated by ^{1}H NMR.
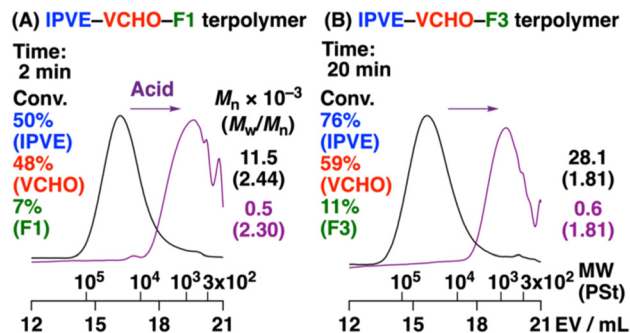
Fig. 4 MWD curves of (A) IPVE–VCHO–F1 and (B) IPVE–VCHO–F3 ter-polymers (black) and their acid hydrolysis products (purple). See Table 4 for the polymerization conditions.

among the three monomers. The terpolymers could be degraded into low-MW compounds by acid *via* the cleavage of the acetal moieties in the main chain (Fig. 4, purple).

The terpolymerization most likely proceeded *via* selective crossover reactions at the VE- and VCHO-derived propagating ends (Scheme 5). The VE-derived carbocation reacted with VE or VCHO, while it did not react with ROFO as expected by ineffective copolymerization of VE and ROFO (Scheme 5A). At the VCHO-derived end, a carbocation was not generated by the ring-opening reaction of the VCHO-derived oxonium ion, resulting in the absence of the reaction with VE (Scheme 5B), as demonstrated by our previous studies.[12,13,27] Accordingly, the VCHO-derived oxonium ion reacted with VCHO or ROFO (Scheme 5B).

We revealed the reaction selectivity at the ROFO-derived propagating end by elaborate analysis of the ^{1}H NMR spectra (Fig. 5). The amounts of homosequence units (IPVE and VCHO) and crossover reaction-derived units (IPVE-to-VCHO, ROFO-to-IPVE, and ROFO-to-VCHO crossover reactions) were calculated by assuming that the amounts of the ROFO-to-IPVE and IPVE-to-VCHO crossover reaction-derived units are the same. For example, from the integral ratios of peaks at 5.6–6.3 (peaks 9, 15, 16, and 18), 4.6–5.4 (peaks 10–12, 14, and 17), 3.0–4.1 (peaks 2, 3, 5, 13, and a), and 2.1–2.5 (peak 8) ppm (Fig. 5A), we concluded that 71% and 29% of the F1-derived propagating species reacted with IPVE and VCHO, respectively (entry 1 in Table 4). Interestingly, this ratio varied among ROFOs (Scheme 5C) and it is most likely that the F3-derived propagating species exclusively reacted with IPVE (>99%/<1% for IPVE/VCHO; entry 3; Fig. 5C; see Fig. S14–S17† for the ^{13}C and 2D NMR spectra). Indeed, peaks assigned to the structures resulting from the degradation of the VCHO–ROFO–VCHO sequence (peaks 25–27) were absent in the ^{1}H NMR spectrum of the degradation product (Fig. 5D), which is in contrast to the F1 counterpart (Fig. 5B). The difference likely stemmed from the stabilities of the acetal moieties resulting from the reaction of the ROFO-derived carbocation and an oxirane. Methoxy, isopropoxy, or *tert*-butoxy group-containing acetal moieties are generated from F1, F2, or F3, respectively. The stability of acetals decreases with an increase in bulkiness of alkoxy groups. Indeed, the acid hydrolysis rates of acetals were
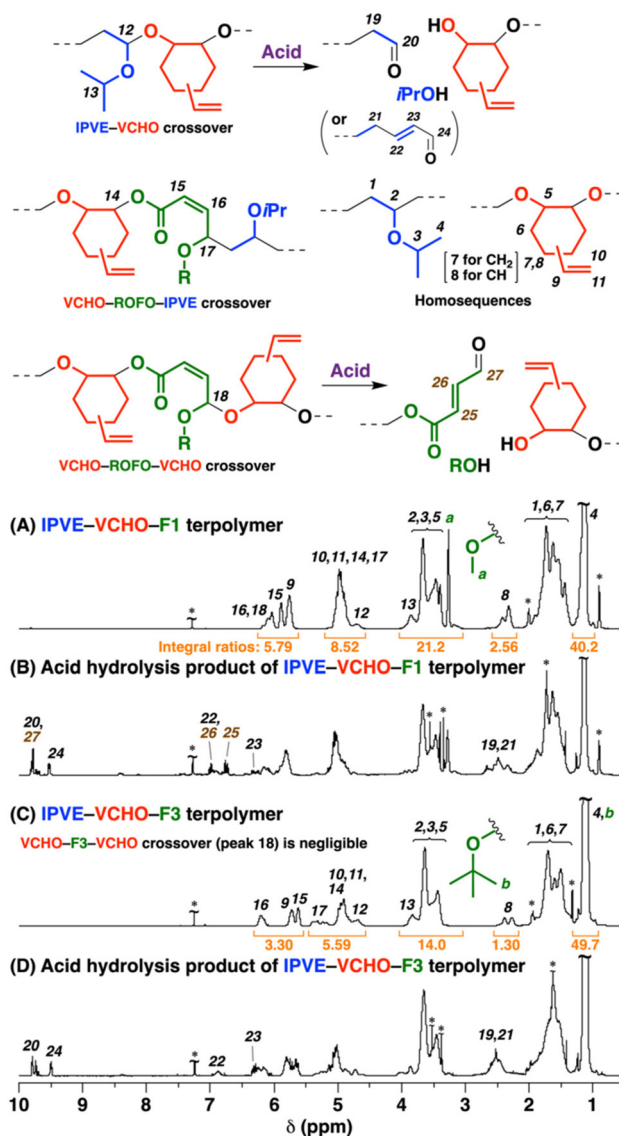

Fig. 5 ^{1}H NMR spectra of (A) IPVE–VCHO–F1 terpolymer (entry 1 in Table 3; Fig. 4A), (B) its acid hydrolysis product (purple curve in Fig. 4A), (C) IPVE–VCHO–F3 terpolymer (entry 3 in Table 3; Fig. 4B), and (D) its acid hydrolysis product (purple curve in Fig. 4B). In CDCl₃ at 30 °C. * CHCl₃, water, 1,2-dimethoxyethane, *etc*.

reported to increase in the order of methoxy < isopropoxy < *tert*-butoxy group-containing acetal.[28] In the terpolymerization, the F3-derived acetal moieties were less favorably generated by the reaction of the F3-derived carbocation with VCHO, resulting in preferential reactions with IPVE, compared to the F1 case. Similar exclusive reactions for VEs rather than oxiranes were observed in the terpolymerization of VE, oxirane, and ROPT in our previous study.[13] The use of ethyl VE, which is a less reactive VE than IPVE, resulted in a terpolymer with shorter VE homosequences (entry 4 in Table 4), while keeping the very high selectivity of the crossover reactions at the F3-derived propagating end (98%/2% for EVE/VCHO). We tried to analyze the terpolymer by MALDI-TOF-MS; however, it was difficult to detect clear peaks because the product is composed
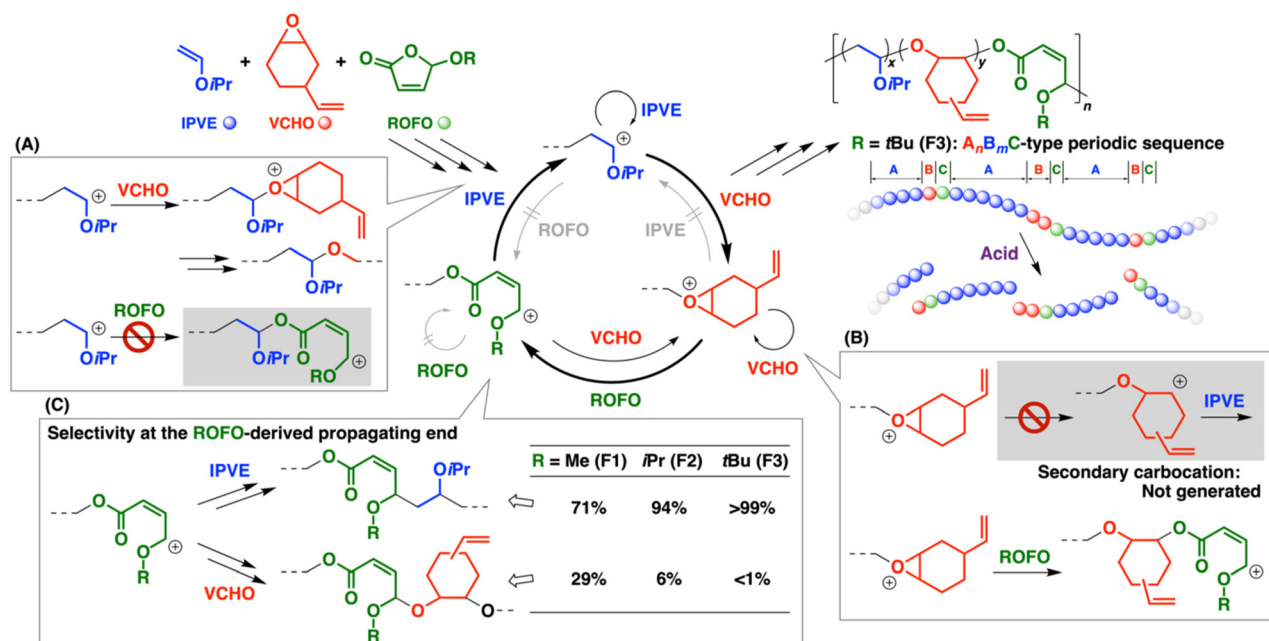
Scheme 5 Cationic terpolymerization of IPVE, VCHO, and ROFO: Propagation reactions at (A) VE-, (B) VCHO, and (C) ROFO-derived propagating ends.

of many polymer chains consisting of the different number of the three monomers (Fig. S18†). Sequences consisting of VCHO–ROFO–IPVE were detected by electrospray ionization mass spectrometry (ESI-MS) analysis of the products obtained by acid hydrolysis of the terpolymers (Fig. S19†).

Cationic alternating copolymerization of vinyl acetate and ROFO

We previously reported that vinyl acetate, which is a cationically nonhomopolymerizable monomer, undergoes cationic alternating copolymerization with DOLOs or ROPTs.[29,30] To examine the potential of ROFOs as comonomers for vinyl acetate, we conducted cationic copolymerization of vinyl acetate and F1 with GaCl$_3$ as a catalyst in dichloromethane at −40 °C. As a result, copolymerization successfully proceeded to yield an alternating copolymer [M_n(GPC) = 5.4 × 10^3; Fig. S20†]. MALDI-TOF-MS analysis also suggested that the copolymer chains had alternating sequences (Fig. S21†).

Thiol–ene reaction of ROFO-derived copolymer

The copolymers obtained from ROFOs have β-substituted acrylate (isocrotonate) moieties in the main chain. To demonstrate functionalization of the β-substituted acrylate moieties, we conducted the thiol–ene reaction[31,32] using 1-dodecanethiol as a model thiol. After the reaction of a CHO–F1 copolymer using 2,2′-azobis(isobutyronitrile) (AIBN) as a radical generator for 24 h, a peak assigned to the methyl group of the 1-dodecanethiol moieties was observed at 0.9 ppm (peak 14 in Fig. 6B) in the ^{1}H NMR spectrum of the product, which indicates the successful incorporation of the thiol by the thiol–ene reaction (incorporated ratio = 40%).
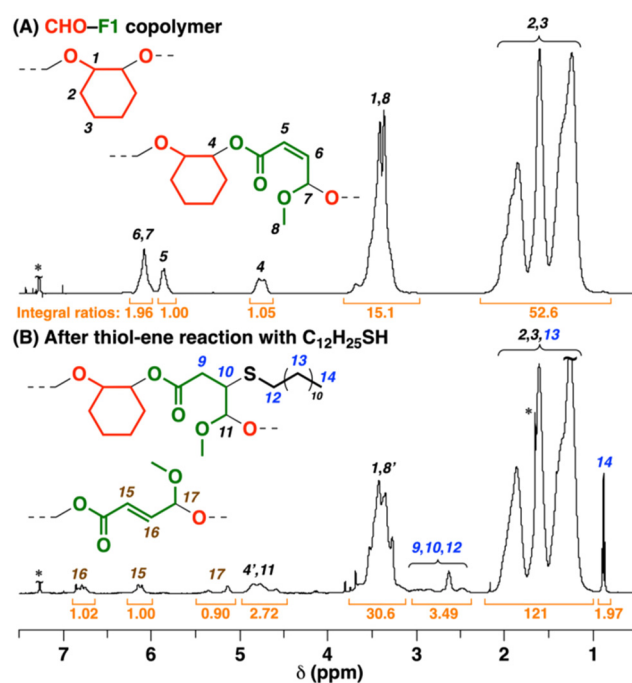

Fig. 6 ^{1}H NMR spectra of (A) CHO–F1 copolymer (obtained under similar conditions to those for entry 1 in Table 3; the average number of CHO/F1 units per block = 6.6/1.0) and (B) the product obtained by the thiol–ene reaction of the copolymer ([double bonds in copolymer]$_0$ = 0.062 M, [C$_{12}$H$_{25}$SH]$_0$ = 0.31 M, [AIBN]$_0$ = 0.031 M, in toluene at 80 °C, 24 h). See Fig. S22† for the MWD curves. * CHCl$_3$ or water.

Interestingly, in the ^{1}H NMR spectra, the peaks of the *cis*-double bonds in the original copolymer (peaks 5 and 6 in Fig. 6A) disappeared, while new peaks emerged at 6.8, 6.1, and

Polymer Chemistry
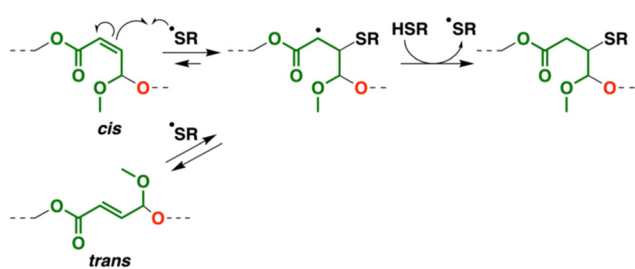
Scheme 6 Thiol–ene reaction and isomerization into *trans*-double bond.

Table 5 T_g values of VCHO–ROFO copolymers and VCHO homopolymer[a]

| Entry | Polymer | Average no. of monomer units per block[b] | | $M_n \times 10^{-3}$[c] | T_g (°C) |
		VCHO	ROFO		
1	VCHO–F1	3.9	1.0	17.8	60
2	VCHO–F2	3.3	1.0	17.8	45
3	VCHO–F3	3.0	1.0	13.8	66
4[d]	VCHO homo	—	—	45.1	50

[a] By DSC (the second heating scan, 10 °C min⁻¹; Fig. S23†). [b] Calculated by ¹H NMR. After purification by preparative GPC (entries 1 and 2) or reprecipitation in methanol (entry 3). [c] Determined by GPC (polystyrene calibration). [d] From ref. 13.

5.1–5.4 ppm (peaks 15–17 in Fig. 6B). These peaks were assigned to *trans*-double bonds,[26] which indicates that the intermediate radical species generated by the reaction of the *cis*-double bond and a thiyl radical underwent the thiyl-radical elimination reaction into not the original *cis*-double bond but a *trans*-double bond during the thiol–ene reaction (Scheme 6).[33]

Thermal properties

The thermal properties of the copolymers consisting of oxiranes and ROFOs were examined by differential scanning calorimetry (DSC). VCHO–F1, VCHO–F2, and VCHO–F3 copolymers exhibited glass transition temperatures (T_gs) of 60, 45, and 66 °C, respectively (entries 1–3 in Table 5, Fig. S23†), which were higher or comparable to the T_g of a VCHO homopolymer (50 °C, entry 4). The difference of the alkoxy groups derived from ROFOs affected the thermal properties of the copolymers. The balance of flexibility and bulkiness of the alkyl substituents likely affected the T_gs. Indeed, the order of the T_gs (substituent: *t*Bu > Me > *i*Pr) is similar to those of poly(alkyl acrylate)s and poly(alkyl methacrylate)s.[34]

Conclusion

In conclusion, ROFOs successfully underwent cationic copolymerization with oxiranes and terpolymerization with VEs and

oxiranes using $B(C_6F_5)_3$ as a catalyst, resulting in acidically degradable polymers. Homopolymerization of ROFOs did not proceed, while copolymerization with oxiranes smoothly proceeded because of the efficient generation of ester and acetal moieties by the crossover reactions between oxiranes and ROFOs. One of the four possible structures, which are related to the conjugated structure and *cis–trans* configuration of the ROFO-derived carbocation, was selectively generated by the crossover reactions from ROFO. The terpolymerization also proceeded *via* the highly selective crossover reactions particularly when F3 was used, resulting in a terpolymer with repetitive IPVE$_n$–VCHO$_m$–F3 sequences. In addition, we could use the ROFO-derived β-substituted acrylate moieties as reaction sites for polymer modification by the thiol–ene reaction. The results obtained in this study will contribute to both understanding the design strategy of nonhomopolymerizable comonomers for cationic copolymerization and developing new degradable polymers from bio-derived monomers.

Conflicts of interest

There are no conflicts to declare.

Data availability

The data supporting this article have been included as part of the ESI.†

Acknowledgements

References

1 S. Penczek and K. Kaluzynski, in *Polymer Science: A Comprehensive Reference*, ed. K. Matyjaszewski and M. Möller, Elsevier B.V., Amsterdam, 2012, Vol. 4.02.

2 P. Kubisa, in *Polymer Science: A Comprehensive Reference*, ed. K. Matyjaszewski and M. Möller, Elsevier B.V., Amsterdam, 2012, Vol. 4.08.

3 S. Penczek, M. Cypryk, A. Duda, P. Kubisa and S. Slomkowski, *Prog. Polym. Sci.*, 2007, **32**, 247–282.

4 J. Herzberger, K. Niederer, H. Pohlit, J. Seiwert, M. Worm, F. Wurm and H. Frey, *Chem. Rev.*, 2016, **116**, 2170–2243.

5 P. Kubisa and J. P. Vairon, in *Polymer Science: A Comprehensive Reference*, ed. K. Matyjaszewski and M. Möller, Elsevier B.V., Amsterdam, 2012, Vol. 4.10.

6 K. Maruyama, A. Kanazawa and S. Aoshima, *Polym. Chem.*, 2019, **10**, 5304–5314.

7 K. Maruyama, A. Kanazawa and S. Aoshima, *Macromolecules*, 2022, **55**, 4034–4045.

8 S. A. Cairns, A. Schultheiss and M. P. Shaver, *Polym. Chem.*, 2017, **8**, 2990–2996.

9 Y. Xu, M. R. Perry, S. A. Cairns and M. P. Shaver, *Polym. Chem.*, 2019, **10**, 3048–3054.

10 R. T. Martin, L. P. Camargo and S. A. Miller, *Green Chem.*, 2014, **16**, 1768–1773.

11 T. Șucu, M. Wang and M. P. Shaver, *Macromolecules*, 2023, **56**, 1625–1632.

12 K. Hyoi, A. Kanazawa and S. Aoshima, *ACS Macro Lett.*, 2019, **8**, 128–133.

13 Y. Takahashi, A. Kanazawa and S. Aoshima, *Macromolecules*, 2023, **56**, 4198–4207.

14 A. E. Neitzel, T. J. Haversang and M. A. Hillmyer, *Ind. Eng. Chem. Res.*, 2016, **55**, 11747–11755.

15 A. E. Neitzel, L. Barreda, J. T. Trotta, G. W. Fahnhorst, T. J. Haversang, T. R. Hoye, B. P. Fors and M. A. Hillmyer, *Polym. Chem.*, 2019, **10**, 4573–4583.

16 M. Okada, H. Sumitomo and Y. Yamamoto, *Makromol. Chem.*, 1974, **175**, 3023–3028.

17 G. O. Schenck, *Justus Liebigs Ann. Chem.*, 1953, **584**, 156–176.

18 J. C. de Jong, F. van Bolhus and B. L. Feringa, *Tetrahedron: Asymmetry*, 1991, **2**, 1247–1262.

19 P. Esser, B. Pohlmann and H.-D. Scharf, *Angew. Chem., Int. Ed. Engl.*, 1994, **33**, 2009–2023.

20 Y. Morita, H. Tokuyama and T. Fukuyama, *Org. Lett.*, 2005, **7**, 4337–4340.

21 J. G. H. Hermens, T. Freese, K. J. van den Berg, R. van Gemert and B. L. Feringa, *Sci. Adv.*, 2020, **6**, eabe0026.

22 M. L. Lepage, G. Alachouzos, J. G. H. Hermens, N. Elders, K. J. van den Berg and B. L. Feringa, *J. Am. Chem. Soc.*, 2023, **145**, 17211–17219.

23 L.-L. Shen, H.-S. Mun and J.-H. Jeong, *Eur. J. Org. Chem.*, 2010, 6895–6899.

24 V. E. Meyer and G. G. Lowry, *J. Polym. Sci., Part A: Gen. Pap.*, 1965, **3**, 2843–2851.

25 N. A. Lynd, R. C. Ferrier Jr and B. S. Beckingham, *Macromolecules*, 2019, **52**, 2277–2285.

26 H.-D. Scharf and J. Janus, *Chem. Ber.*, 1978, **111**, 2741–2744.

27 M. Mimura, A. Kanazawa and S. Aoshima, *Macromolecules*, 2019, **52**, 7572–7583.

28 A. T. N. Belarmino, S. Froehner, D. Zanette, J. P. S. Farah, C. A. Bunton and L. S. Romsted, *J. Org. Chem.*, 2003, **68**, 706–717.

29 J. Azuma, A. Kanazawa and S. Aoshima, *Macromolecules*, 2022, **55**, 6110–6119.

30 K. Kamigaki, S. Aoshima and A. Kanazawa, *ACS Macro Lett.*, 2024, **13**, 754–760.

31 B. H. Northtop and R. N. Coffey, *J. Am. Chem. Soc.*, 2012, **134**, 13804–13817.

32 Y. Yu, M. Kim, G. S. Lee, H. W. Lee, J. G. Kim and B.-S. Kim, *Macromolecules*, 2021, **54**, 10903–10913.

33 C. Walling and W. Helmreich, *J. Am. Chem. Soc.*, 1959, **81**, 1144–1148.

34 R. J. Andrews and E. A. Grulke, in *Polymer Handbook*, Fourth Edition, ed. J. Brandrup, E. H. Immergut and E. A. Grulke, Wiley-Interscience, 1999, ch. VI, p. 193.